Advanced Gel Electrophoresis Techniques Reveal Heterogeneity of Humic Acids Based on Molecular Weight Distributions of Kinetically Inert Cu^{2+}-Humate Complexes

Kazuki Marumo,[†] Atsumasa Matsumoto,[†] Sumika Nakano,[†] Masami Shibukawa, [†] Takumi Saito,[‡] Tomoko Haraga,[¶] and Shingo Saito [†,]*

[†]Graduate School of Science and Engineering, Saitama University, 255 Shimo-Okubo, Sakura-ku, Saitama 338-8570, Japan

[‡]Graduate School of Engineering, Tokyo University, 7-3-1 Hongo, Bunkyo-ku, Tokyo 113-8656, Japan

[¶]Department of Decommissioning and Waste Management, Japan Atomic Energy Agency, 2-4 Shirakata, Tokai-mura, Naka-gun, Ibaraki 319-1195, Japan

17 pages, including 1 table and 9 figures

Contents

1. Other chemicals and instruments

A MW protein standard (3-color Prestained XL-Ladder, Apro Science, Tokushima, Japan) was used as a MW marker. Solutions of 10% ammonium persulfate (APS; Kishida Chemical Co. Ltd., Osaka, Japan) and *N,N,N′,N′*-tetramethylethylenediamine (TEMED; Acros Organics, Geel, Belgium), used for acceleration of polymerization, were prepared at the time of use.

A thermostatted water bath (LTB-125, AS ONE, Osaka, Japan) and an incubator (MIR-252, SANYO Electric, Osaka, Japan) were employed to control the temperature of the slab gels.

2. Results

Table S1. Characterization of humic acids employed in this study.[1]

Name	Origin of HA	Elemental composition(%)					13C NMR carbon distribution (%)				Acidic functional group (mmol/g)		
		Ash	C	H	O	N	carbonyl	carboxyl	aromatic	aliphatic	carboxyl	phenol	nitirogen-bearing
PAHA	Peat	1	56	5	39	1	4	16	56	24	8.04	3.84	0.77
DHA	Forest soil	1	53	5	37	4	3	11	33	30	8.07	3.16	6.05
IHA	Volcanic ash soil	1	55	4	37	4	4	15	37	23	7.68	3.46	5.22
LHA	Lignite	3	64	4	31	1	8	15	58	15	7.46	2.31	1.38

1) S. Lukman et al., *Geochimica et Cosmochimica Acta*, 2012, **88**, 199–215.

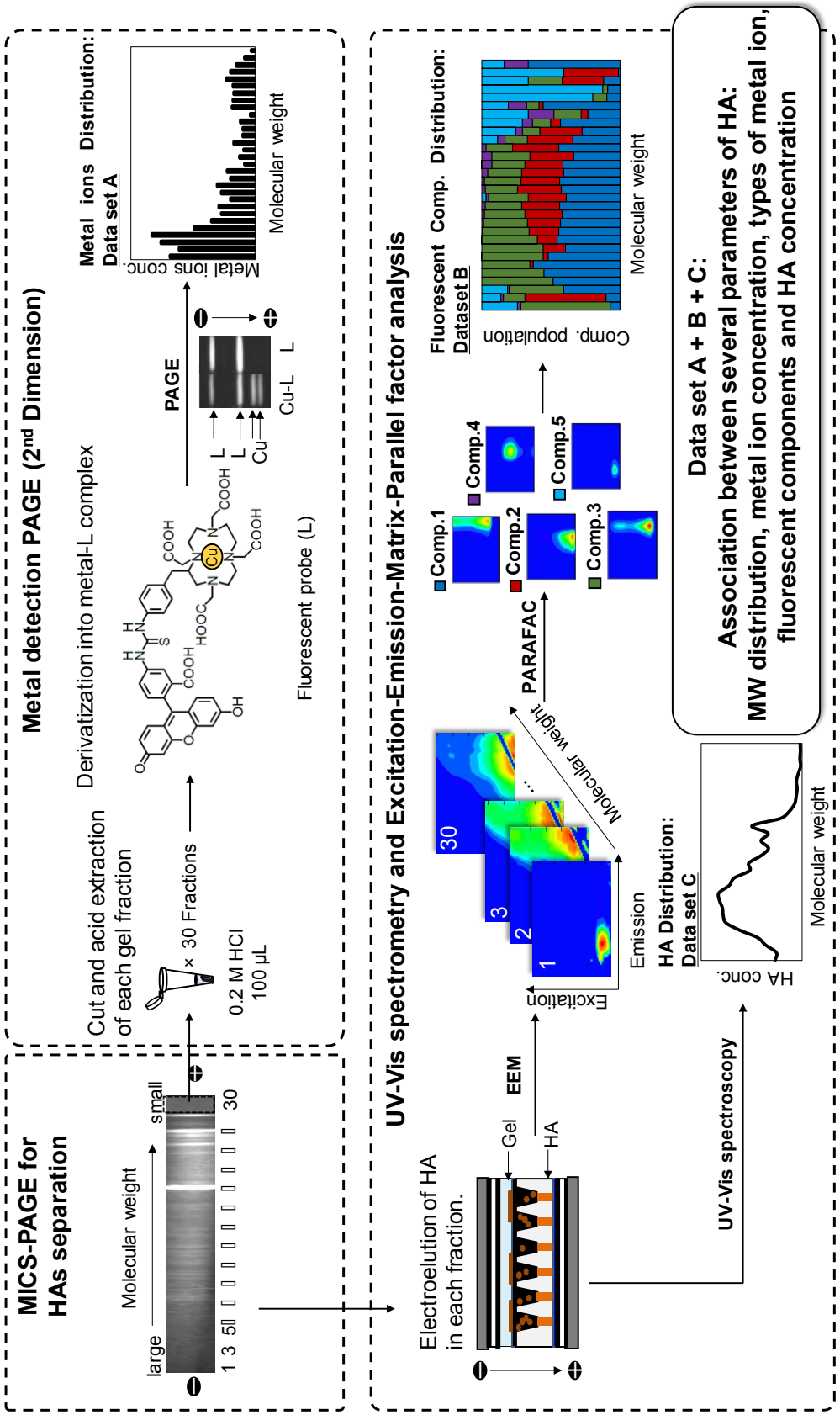

Figure S1. Outline of our MICS-PAGE/metal-detection PAGE/UV-Vis/EEM-PARAFAC methodology.

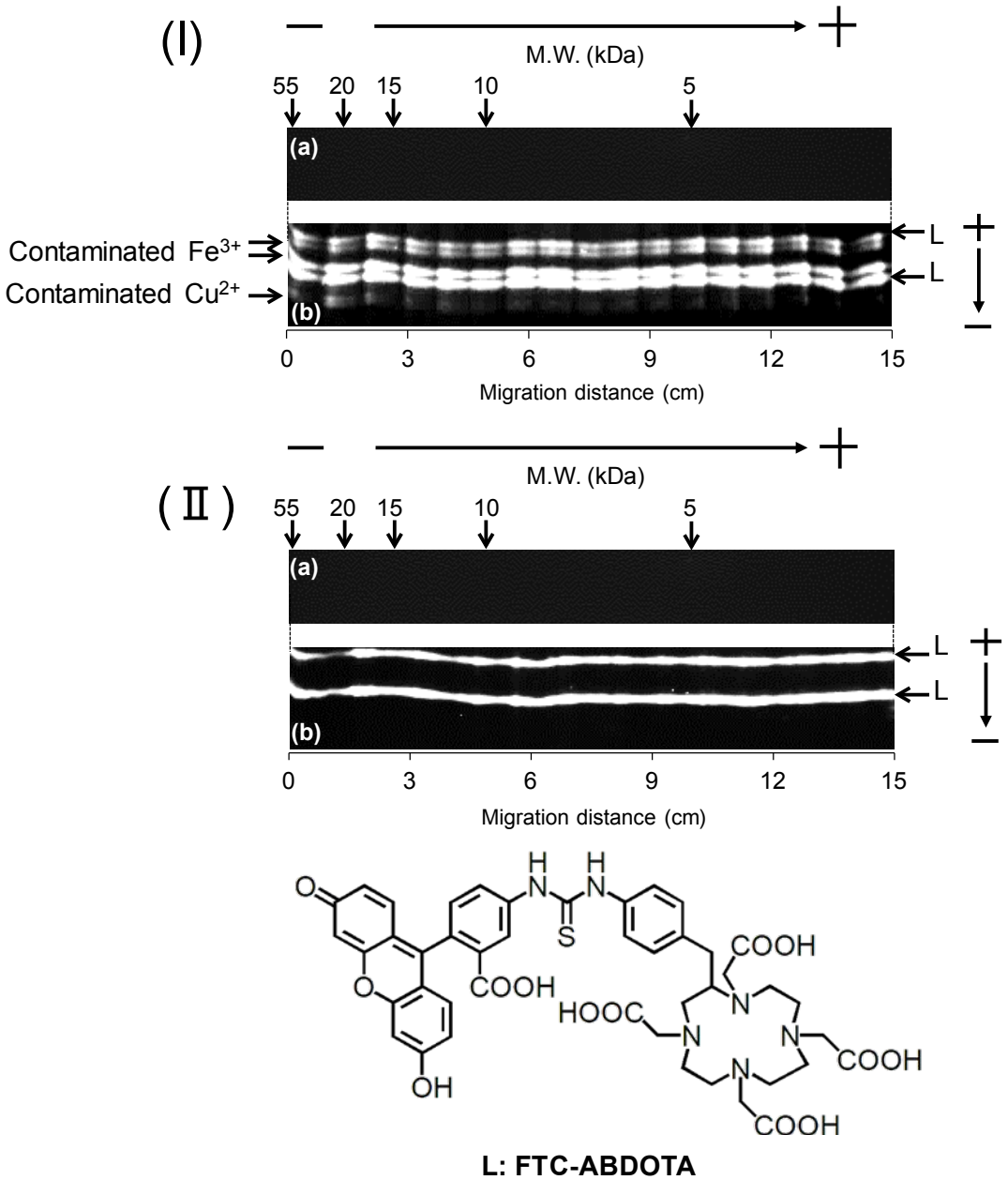

Figure S2. Electropherograms for HA separation PAGE (a) and metal-detection PAGE (b) for an ultrapure water sample: (I) conventional PAGE without the MICS mode and (II) MICS-PAGE. Fe–L: fluorescence bands of Fe^{3+}–FTC-ABDOTA complex, Cu–L: fluorescence bands of Cu^{2+}–FTC-ABDOTA complex, L: fluorescence bands of free FTC-ABDOTA.

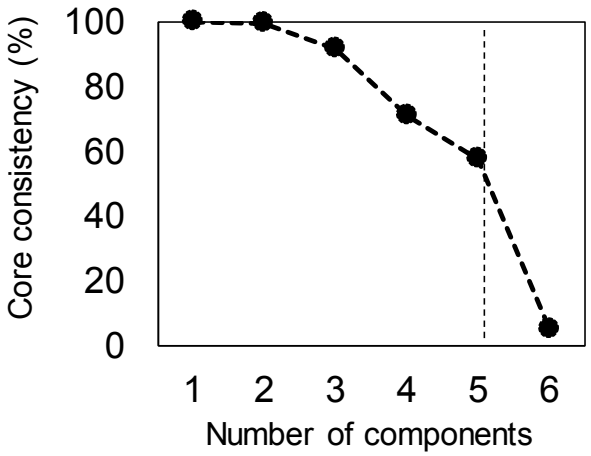

Figure S3. Core consistency as a function of the number of components in PARAFAC modeling.

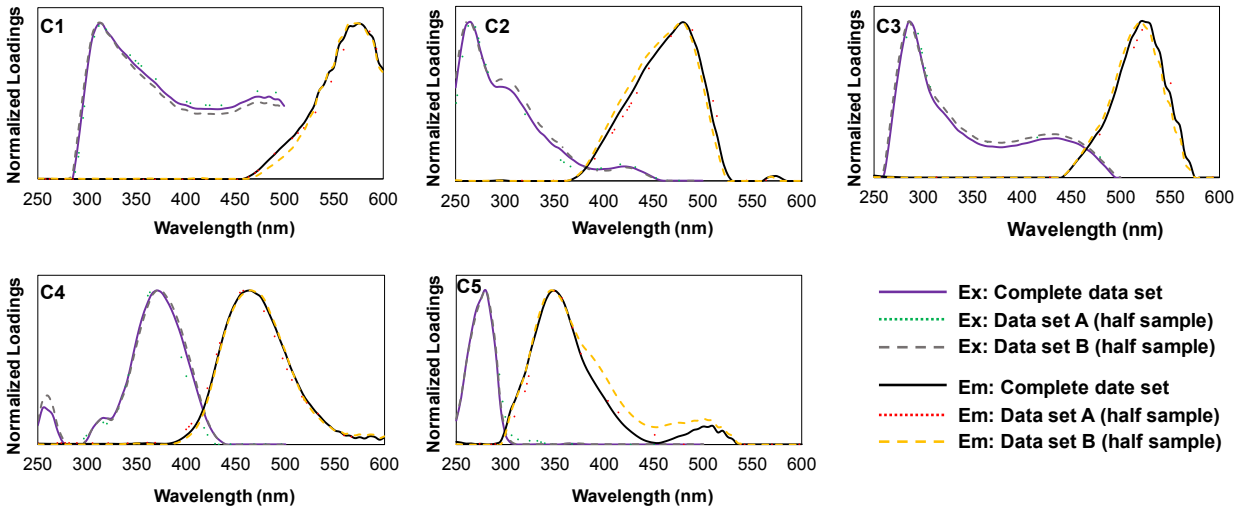

Figure S4. Results of the split-half analysis of our data sets. The split-half was performed by dividing the complete data set into two subsets depending on the origin and addition of Cu^{2+}; Data set A consist of PAHA, Cu^{2+}−DHA, Cu^{2+}−IHA and LHA. Data set B consist of Cu^{2+}−PAHA, DHA, IHA, and Cu^{2+}−LHA.

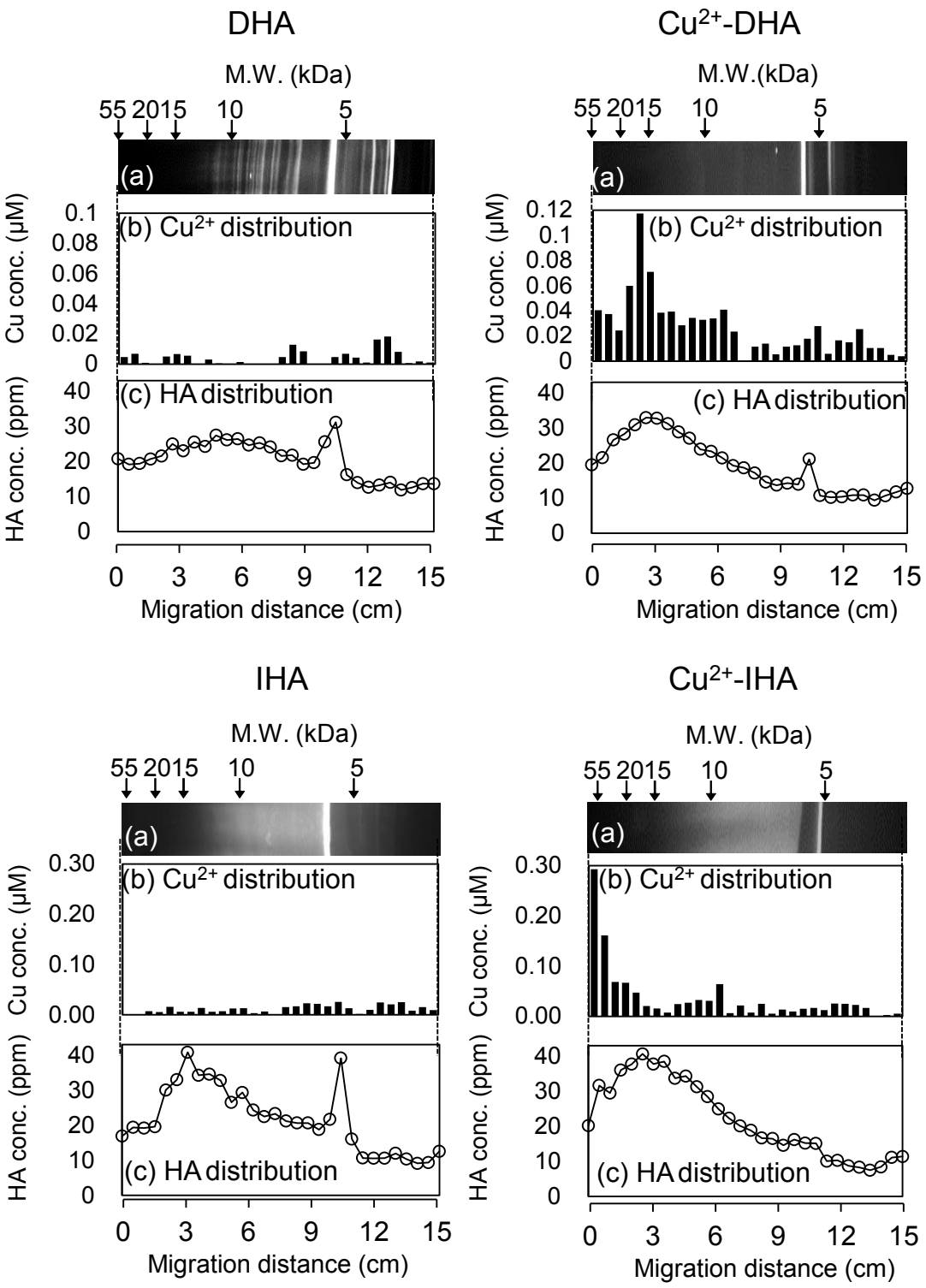
DHA
Cu2+-DHA
IHA
Cu2+-IHA
M.W. (kDa)
55 20 15 10 5
(a)
(b) Cu2+ distribution
(c) HA distribution
Cu conc. (μM)
HA conc. (ppm)
Migration distance (cm)
0 3 6 9 12 15

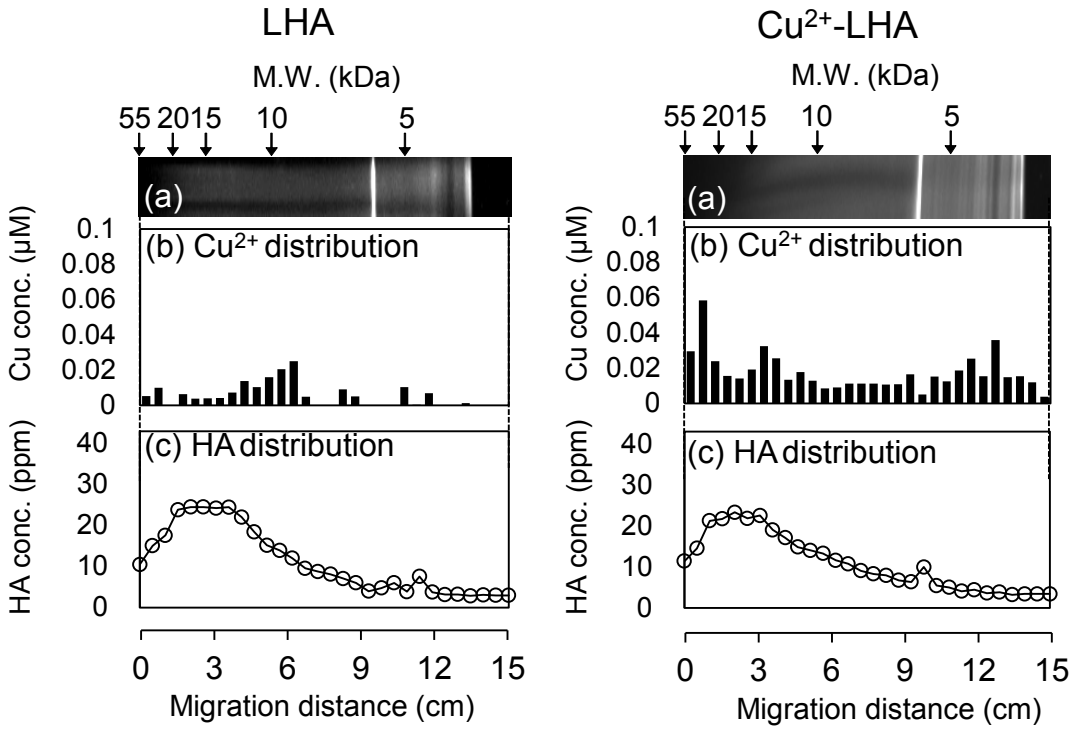

Figure S5. Typical MW distributions of Cu^{2+} for each DHA, IHA, and LHA without (left) or with added Cu^{2+} (right). (a) Electropherograms with fluorescence detection, (b) Cu^{2+} distributions measured by metal-detection PAGE, and (c) HA distributions measured by UV-Vis spectroscopy. Sample: [HA] = 50 ppm, $[Cu^{2+}]$ = 0 or 4 μM, [Tris-HCl] = 60 mM, pH 7.4.

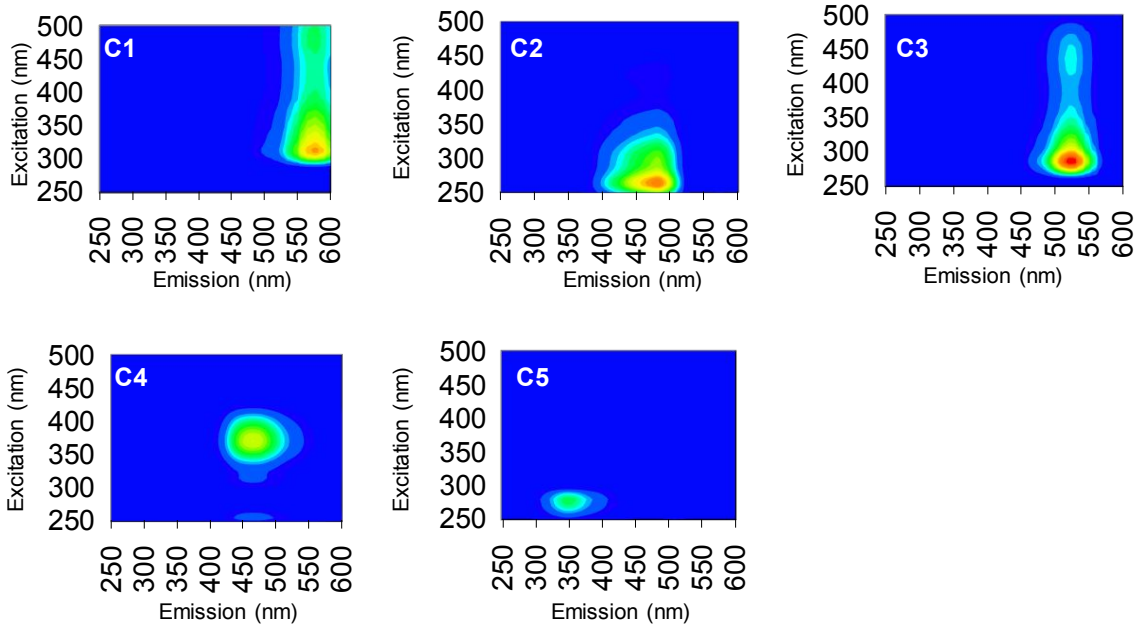

Figure S6. EEM spectra of the five florescent components obtained by MICS-PAGE/EEM-PARAFAC.

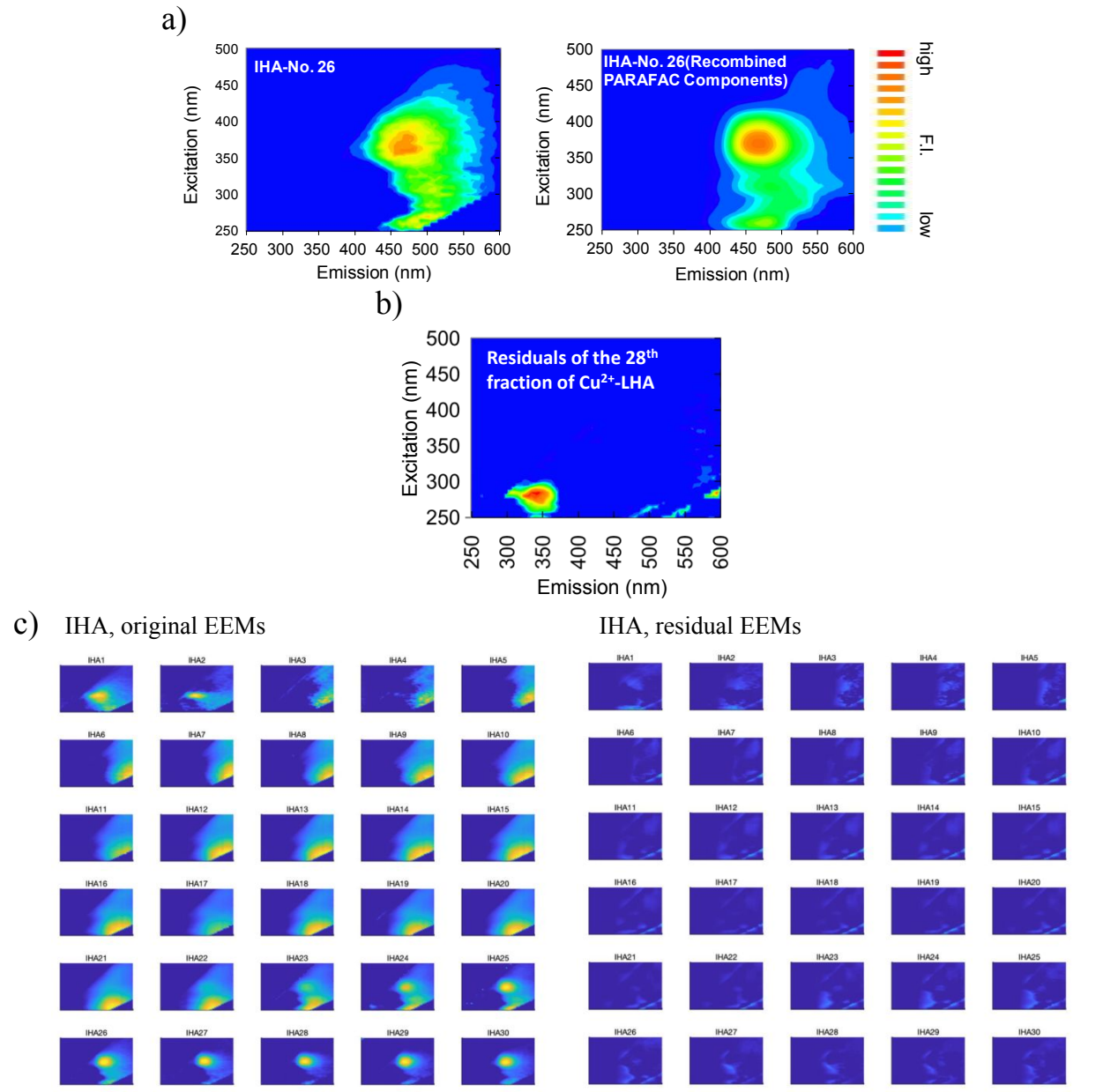

Figure S7. EEM spectrum of the 26th MW fraction of an IHA sample (a, left) and EEM spectrum obtained by recombining the five PARAFAC components for this fraction (a, right), a residual EEM of the 28th fraction of Cu^{2+}-LHA using four-component PARAFAC model (b), and residual EEMs compared with original EEMs for IHA (c). The residual EEM in (b) showed protein-like component was significantly observed as residual error.

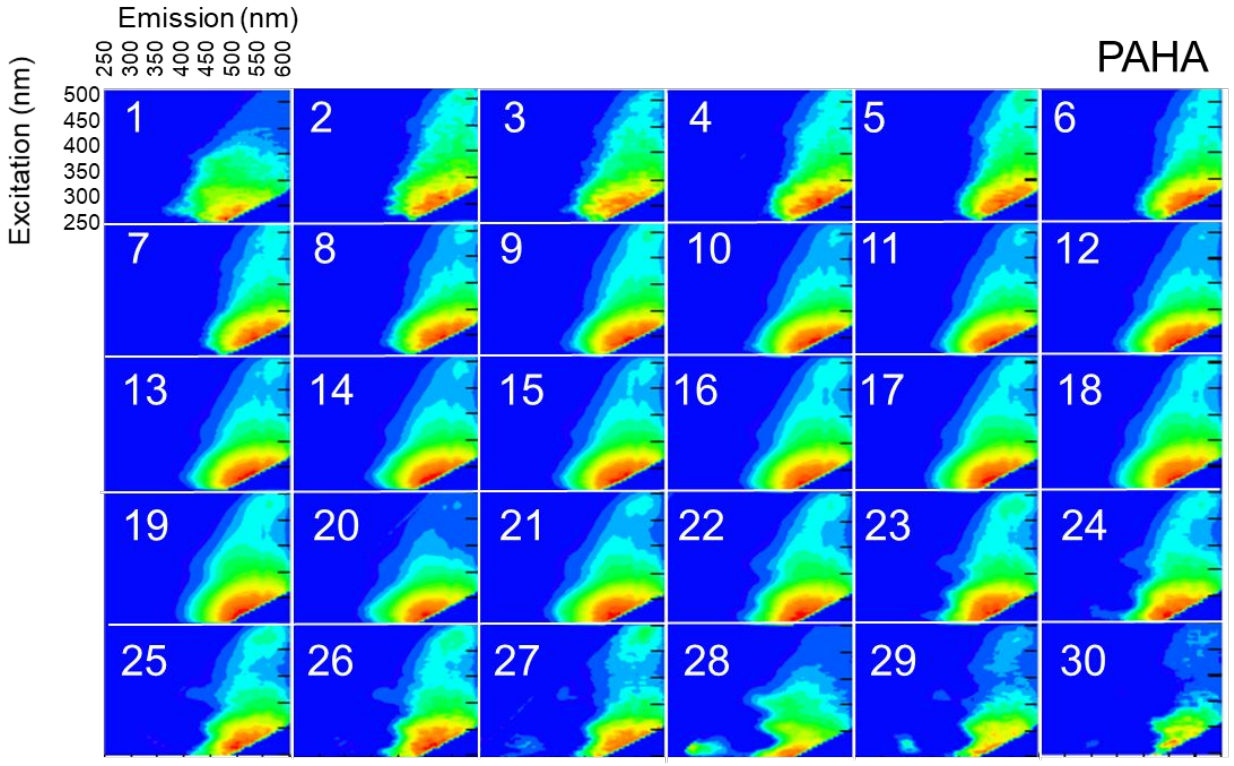
Emission (nm)
250 300 350 400 450 500 550 600
Excitation (nm)
500 450 400 350 300 250
PAHA
1 2 3 4 5 6
7 8 9 10 11 12
13 14 15 16 17 18
19 20 21 22 23 24
25 26 27 28 29 30

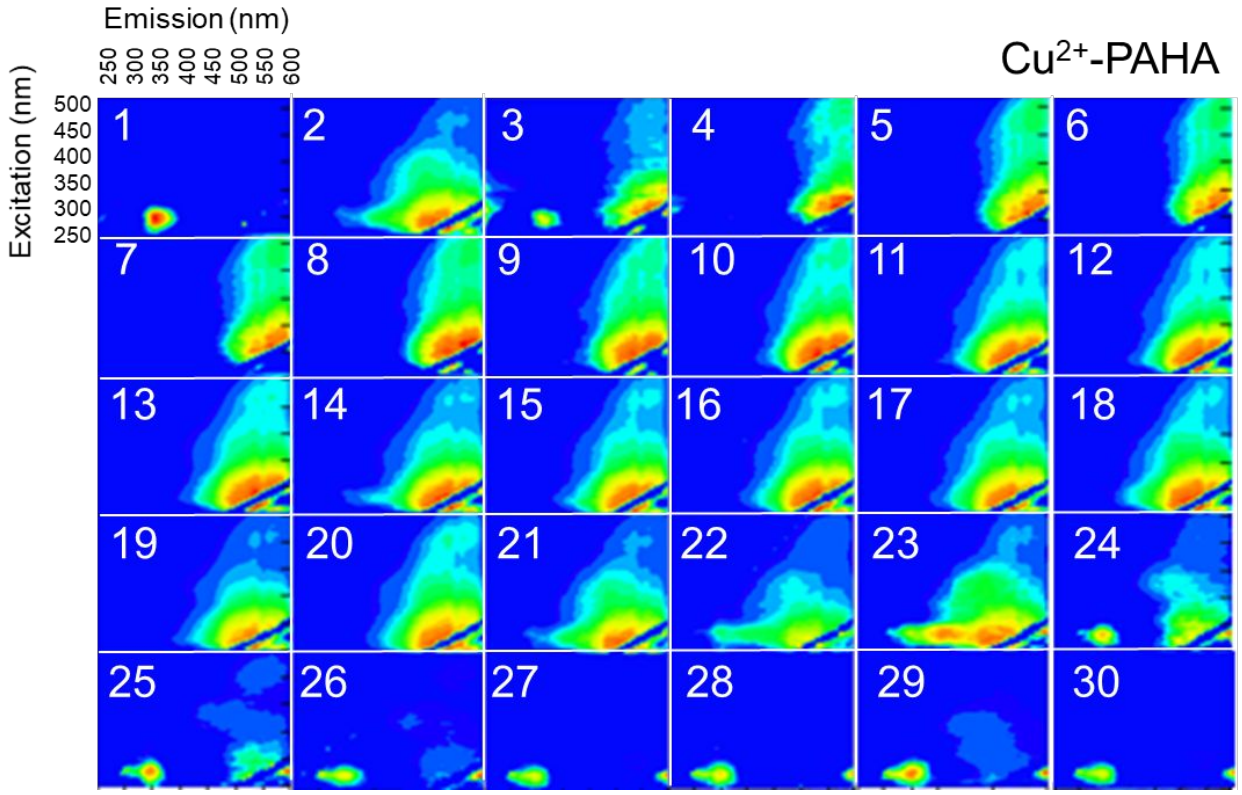
Emission (nm)
250 300 350 400 450 500 550 600
Excitation (nm)
500 450 400 350 300 250
Cu2+-PAHA
1 2 3 4 5 6
7 8 9 10 11 12
13 14 15 16 17 18
19 20 21 22 23 24
25 26 27 28 29 30

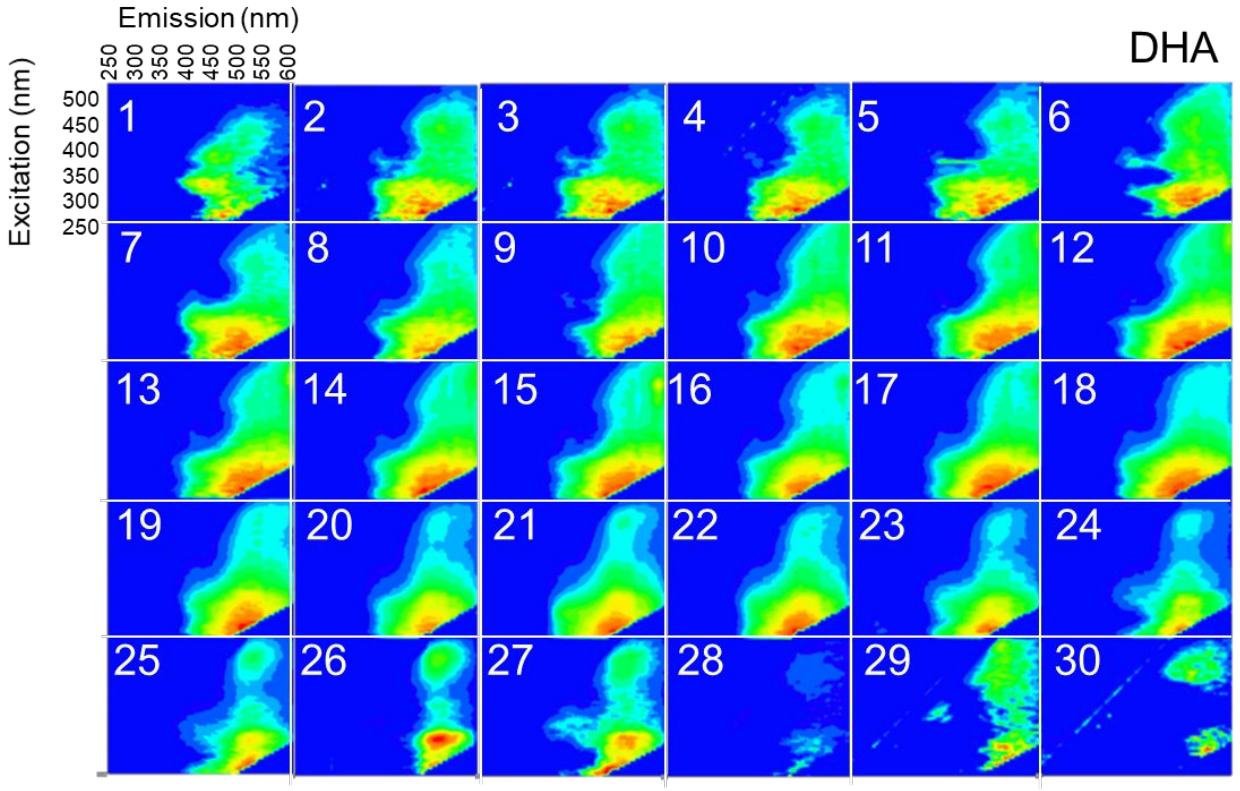
DHA
Emission (nm)
250 300 350 400 450 500 550 600
Excitation (nm)
500 450 400 350 300 250
1 2 3 4 5 6
7 8 9 10 11 12
13 14 15 16 17 18
19 20 21 22 23 24
25 26 27 28 29 30

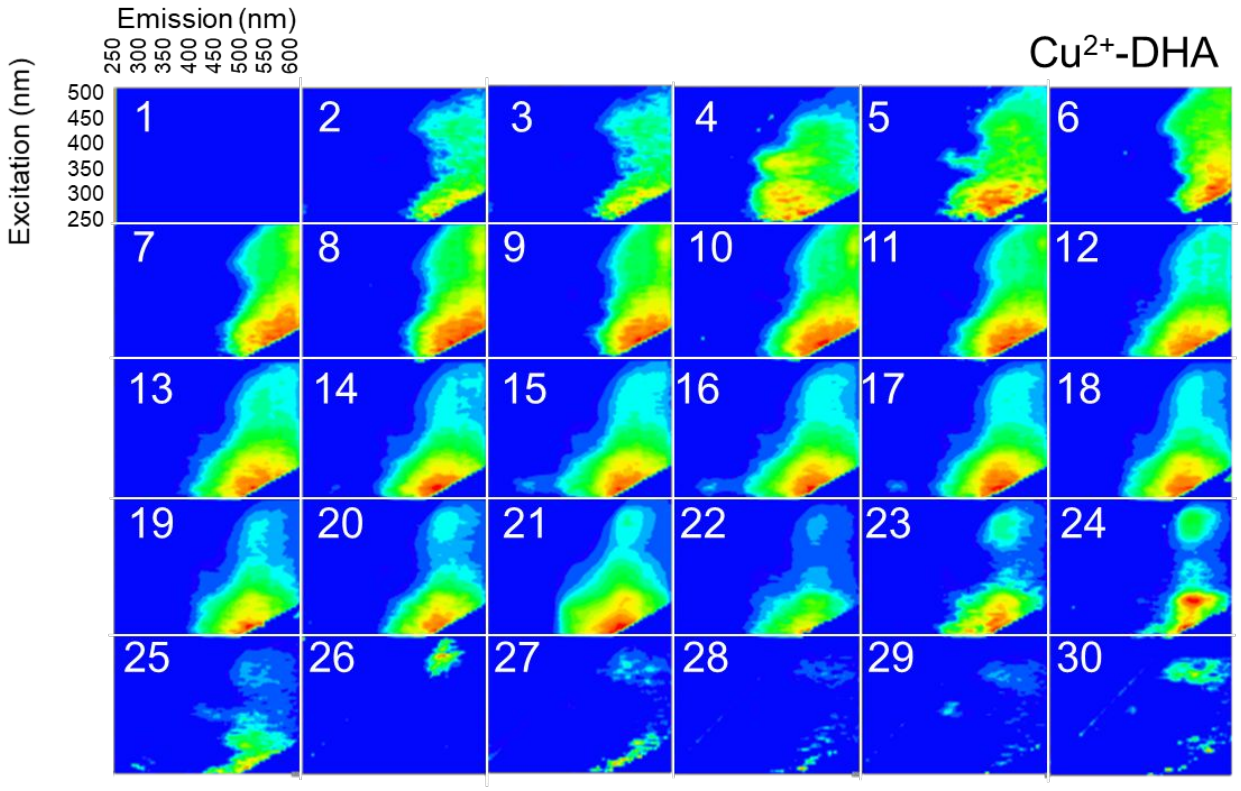
Cu2+-DHA
Emission (nm)
250 300 350 400 450 500 550 600
Excitation (nm)
500 450 400 350 300 250
1 2 3 4 5 6
7 8 9 10 11 12
13 14 15 16 17 18
19 20 21 22 23 24
25 26 27 28 29 30

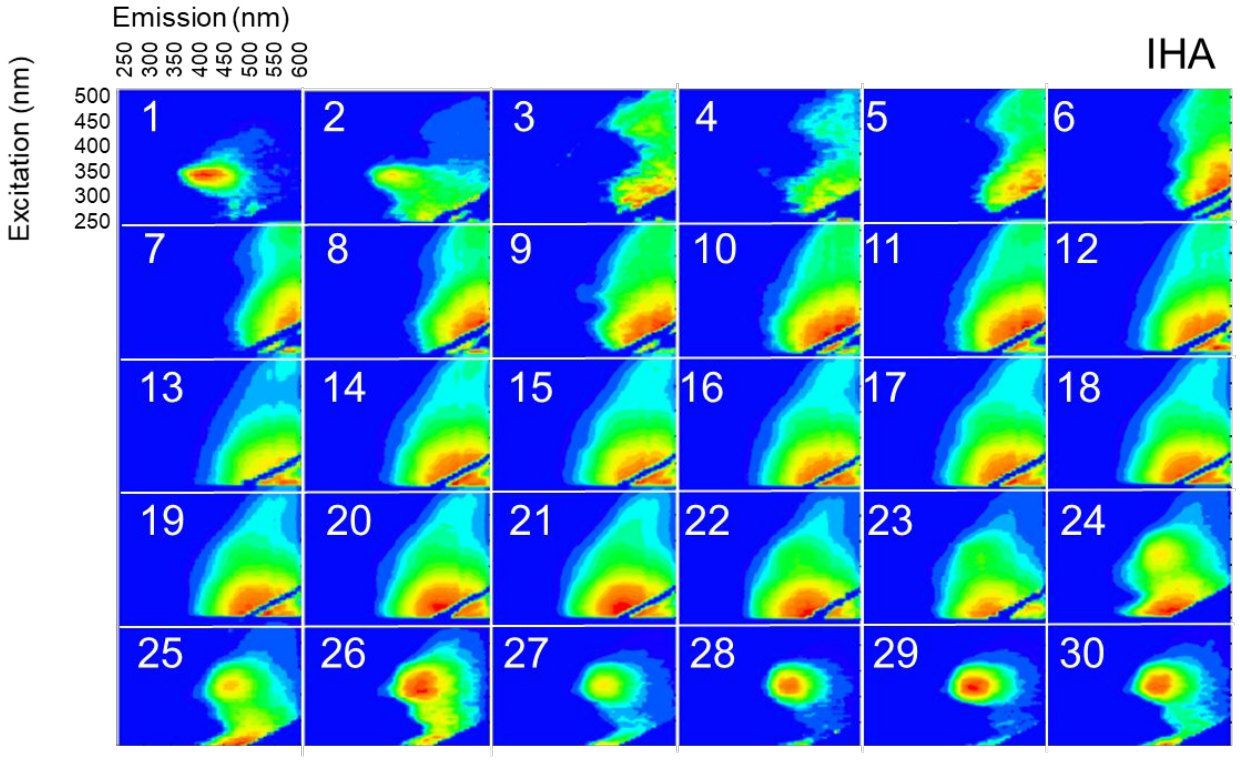
Emission (nm)
250 300 350 400 450 500 550 600
Excitation (nm)
500 450 400 350 300 250
IHA
1 2 3 4 5 6
7 8 9 10 11 12
13 14 15 16 17 18
19 20 21 22 23 24
25 26 27 28 29 30

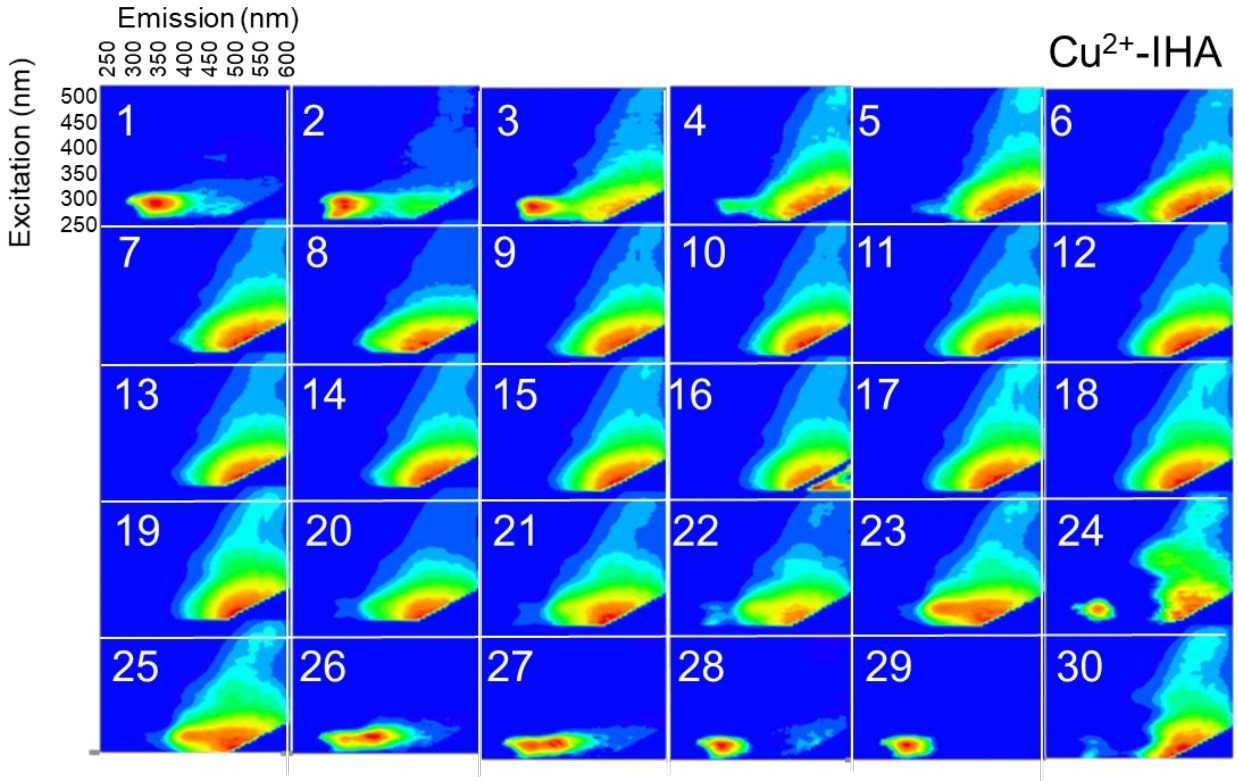
Emission (nm)
250 300 350 400 450 500 550 600
Excitation (nm)
500 450 400 350 300 250
Cu2+-IHA
1 2 3 4 5 6
7 8 9 10 11 12
13 14 15 16 17 18
19 20 21 22 23 24
25 26 27 28 29 30

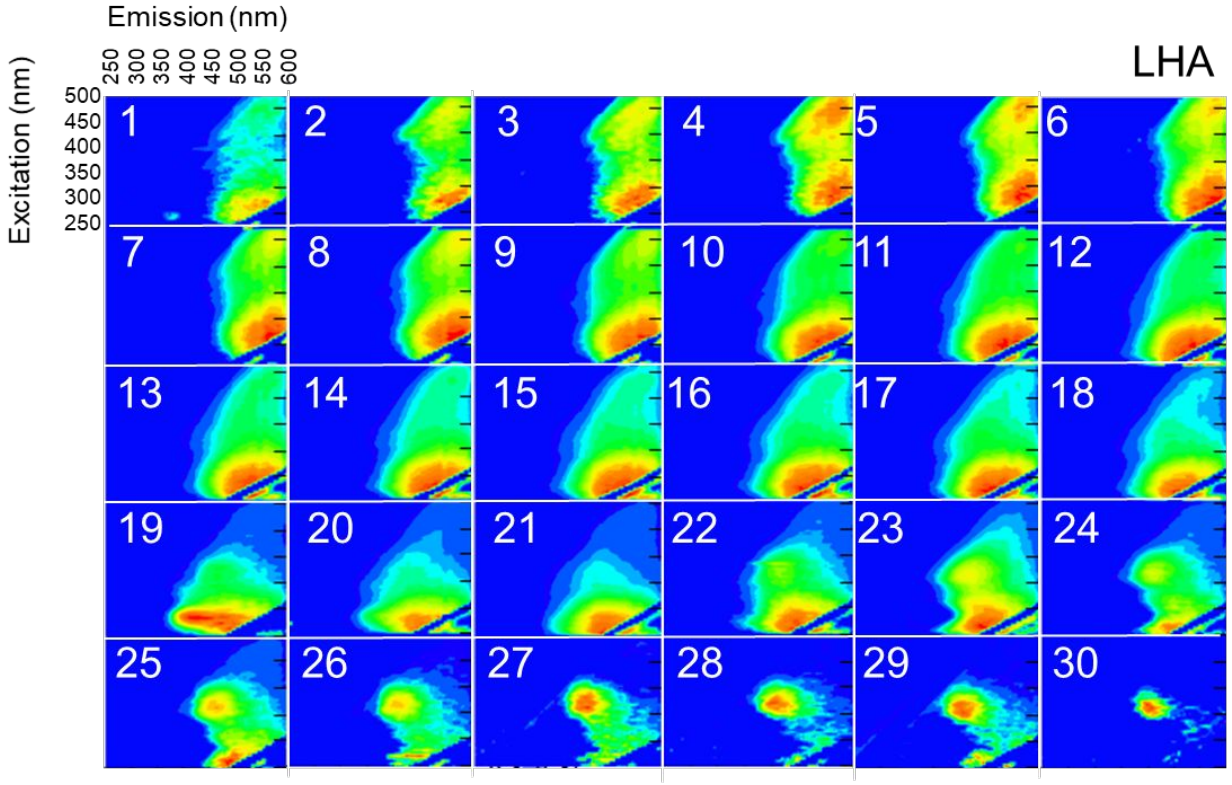
Emission (nm)
250 300 350 400 450 500 550 600
Excitation (nm)
500 450 400 350 300 250
LHA
1 2 3 4 5 6
7 8 9 10 11 12
13 14 15 16 17 18
19 20 21 22 23 24
25 26 27 28 29 30

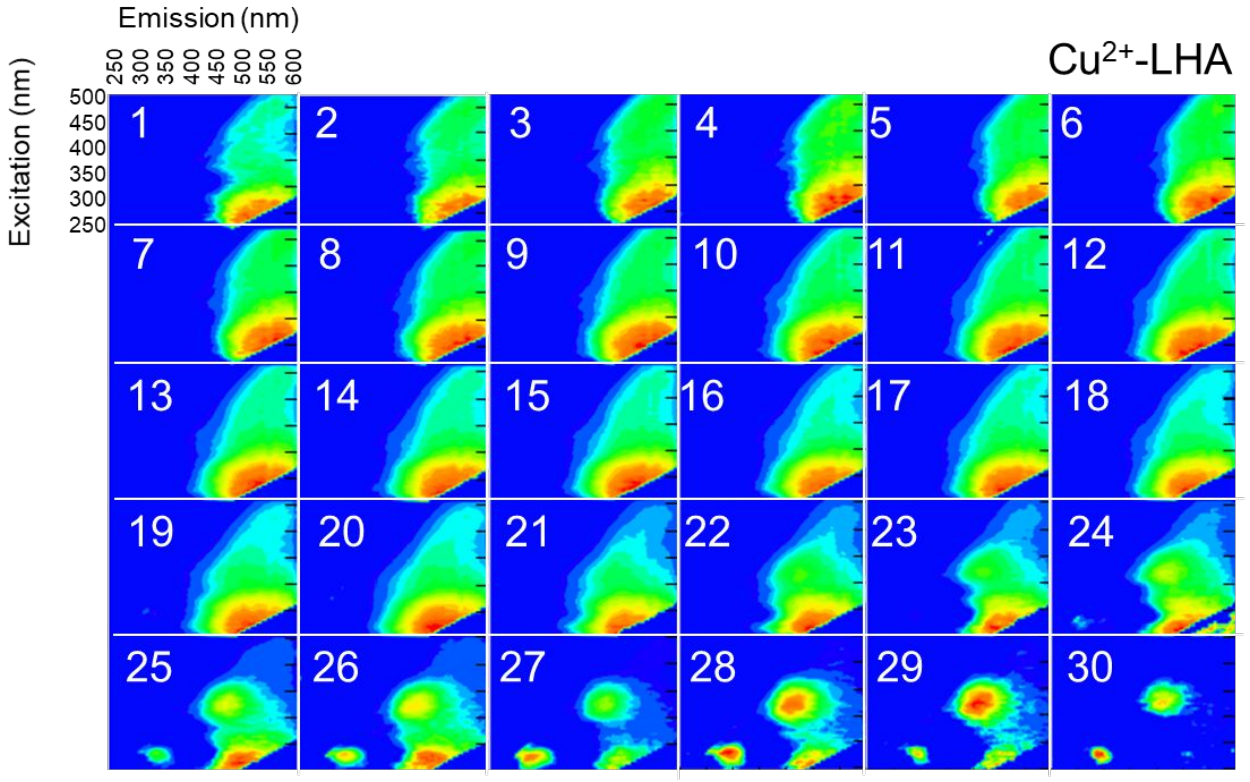

Figure S8. EEM spectra for HAs and Cu^{2+}-HA complexes for PAHA, DHA, IHA, and LHA.

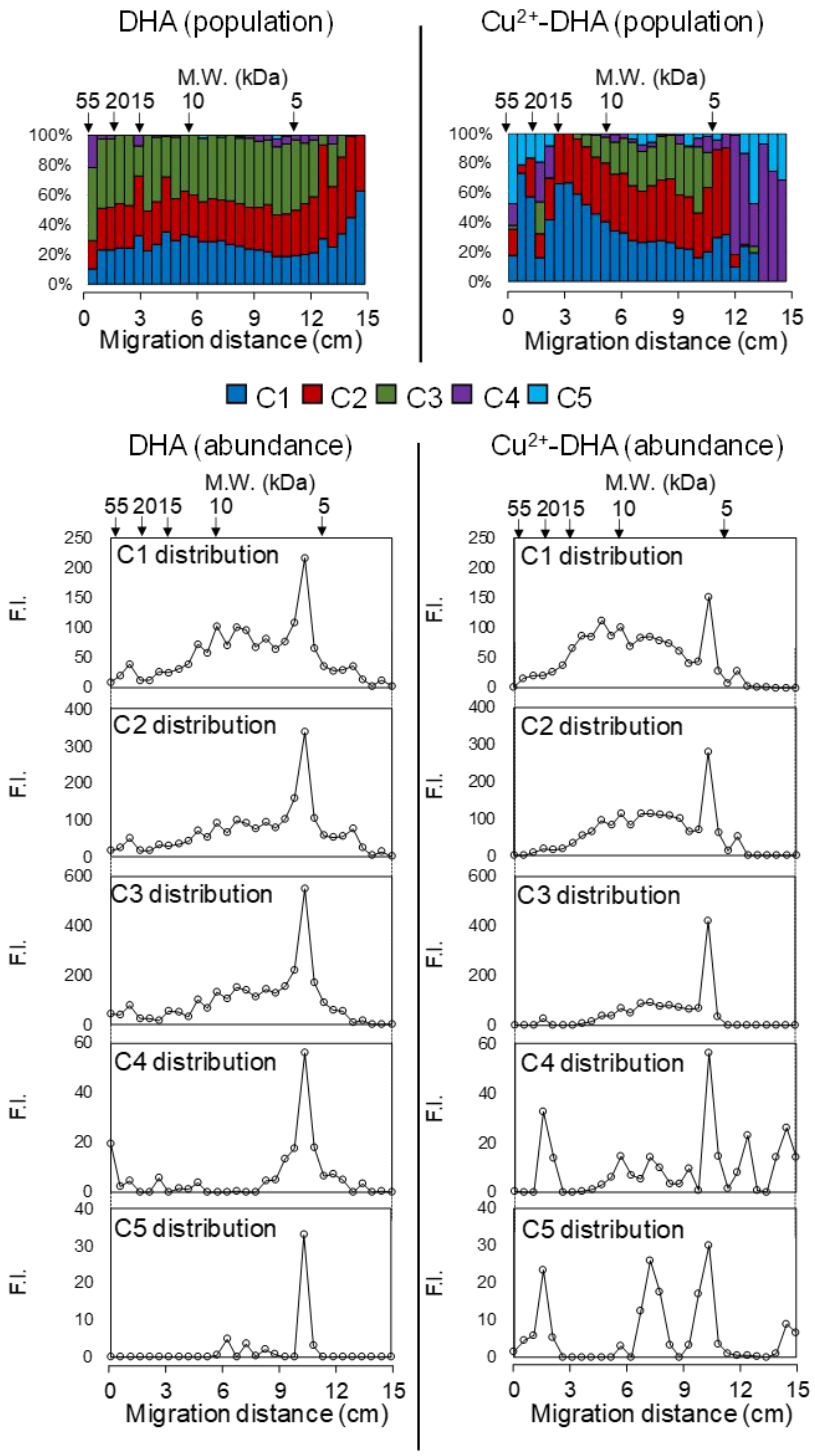
DHA (population)
Cu2+-DHA (population)
M.W. (kDa)
55 20 15 10 5
100%
80%
60%
40%
20%
0%
0 3 6 9 12 15
Migration distance (cm)
C1 C2 C3 C4 C5
DHA (abundance)
Cu2+-DHA (abundance)
C1 distribution
C2 distribution
C3 distribution
C4 distribution
C5 distribution
F.I.

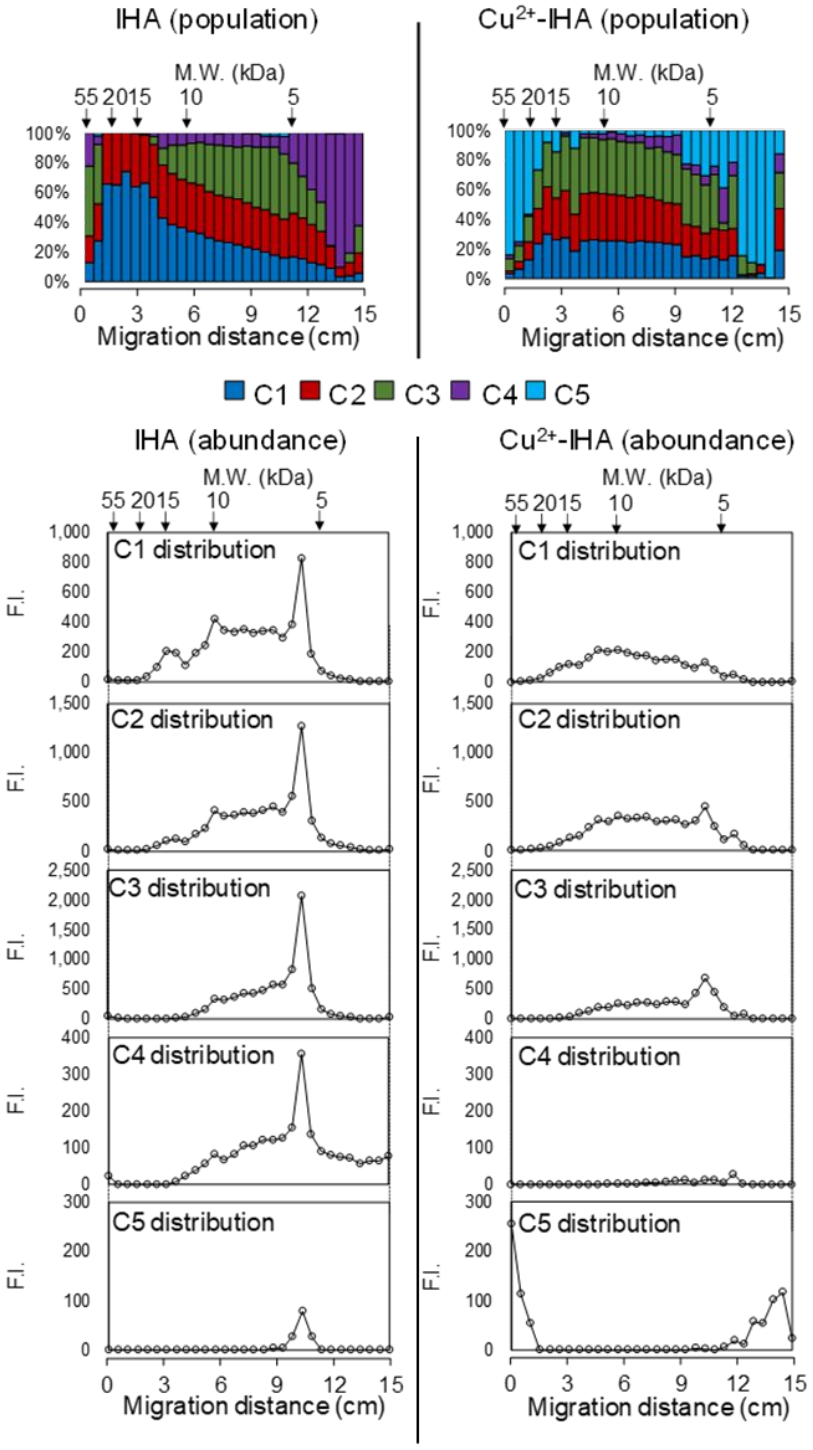
IHA (population)
Cu2+-IHA (population)
M.W. (kDa)
55 20 15 10 5
100%
80%
60%
40%
20%
0%
0 3 6 9 12 15
Migration distance (cm)
C1 C2 C3 C4 C5
IHA (abundance)
Cu2+-IHA (aboundance)
C1 distribution
C2 distribution
C3 distribution
C4 distribution
C5 distribution
F.I.

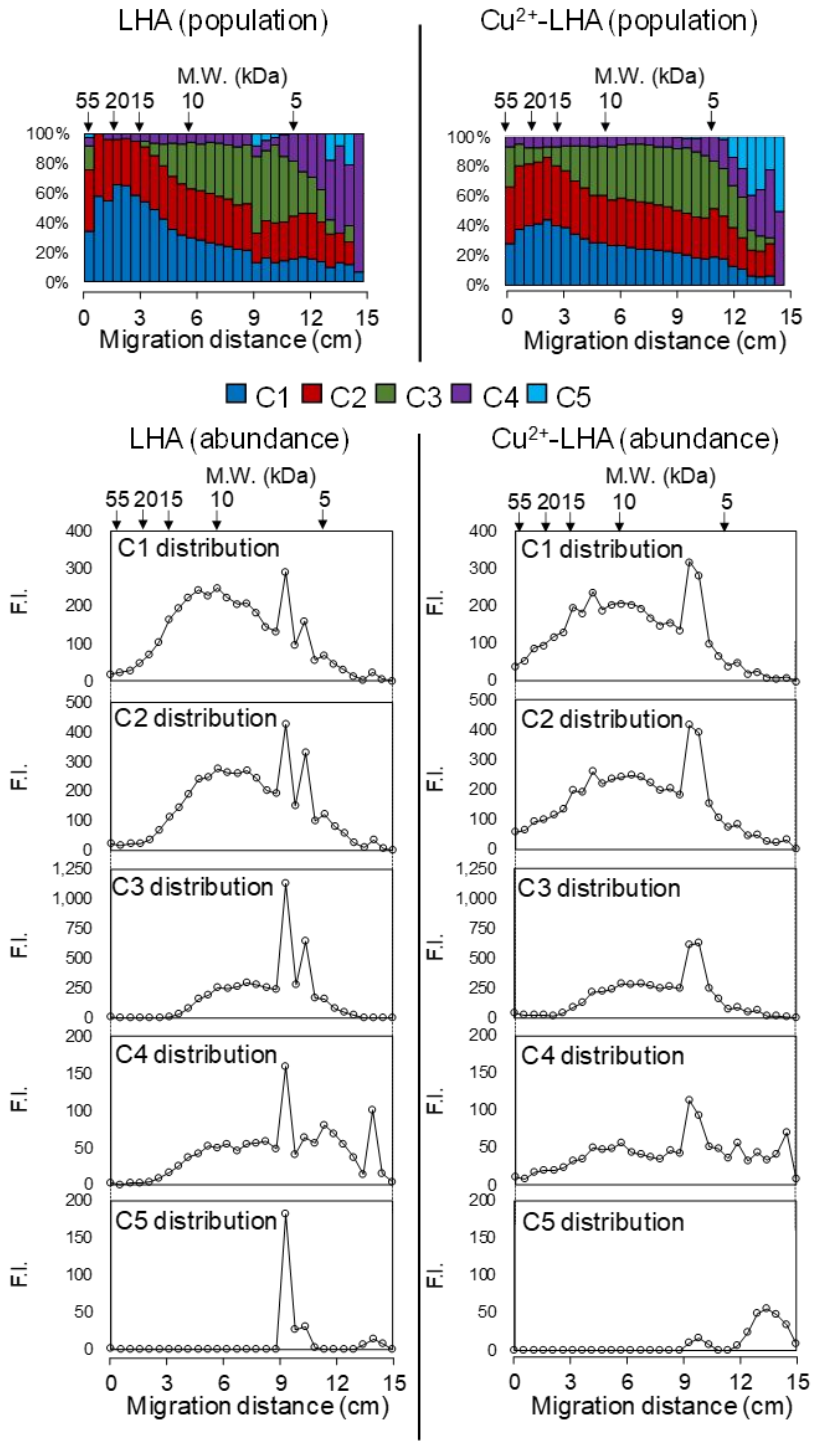

Figure S9. Populations and abundances of the five fluorescent components in each MW fraction for DHA, IHA, LHA, Cu^{2+}–DHA, Cu^{2+}–IHA, and Cu^{2+}–LHA.